Journal of Clinical and Translational Hepatology **2025**
DOI: 10.14218/JCTH.2025.00213

Original Article

Oxytocin Attenuates Metabolic Dysfunction-associated Steatotic Liver Disease via AMPK/SREBP1c/FAS-mediated Suppression of Hepatic Lipogenesis

Yue Xu[1,2#], Siqian Lu[1#], Hongpei Wu[1], Haifeng Wu[1], Ming Li[1,3], Meng Zhou[1], Ting Chen[1], Xun Wang[1], Lishuai Qu[1], Qin Jin[4*] and Jinxia Liu[1*]

[1]Department of Gastroenterology, Affiliated Hospital of Nantong University, Nantong, Jiangsu, China; [2]Department of Hepatology, The Fifth People's Hospital of Suzhou, Suzhou, Jiangsu, China; [3]Dalian Medical University, Dalian, Liaoning, China; [4]Department of Pathology, Affiliated Hospital of Nantong University, Nantong, Jiangsu, China

Received: May 09, 2025 | **Revised:** September 03, 2025 | **Accepted:** November 06, 2025 | **Published online:** November 26, 2025

Abstract

Background and aims: As the leading cause of chronic liver disease globally, metabolic dysfunction-associated steatotic liver disease (MASLD) lacks effective therapies. This study aimed to investigate the therapeutic potential and molecular mechanisms of oxytocin (OXT) in MASLD. ***Methods:*** Integrated bioinformatics analysis of MASLD datasets was carried out to identify OXT-related metabolic disturbances. Serum OXT levels were quantified using an enzyme-linked immunosorbent assay in 113 MASLD patients and 63 healthy controls. Mechanistic assays were conducted using oleic acid (OA)-induced, lipid-loaded HepG2 cells and high-fat diet-fed C57BL/6 mice, and OXT was administered intraperitoneally *in vivo* and supplemented *in vitro*. ***Results:*** Bioinformatics analysis revealed significant changes in OXT expression levels, particularly in fatty acid metabolism. Elevated OXT expression levels in MASLD patients were identified as an independent prognostic factor. *In vitro*, OXT significantly reduced OA-induced lipid accumulation in HepG2 cells, while *in vivo*, it decreased body weight, liver injury, and serum cholesterol levels in high-fat diet-fed mice. Mechanistically, OXT enhanced the expression level of phosphorylated AMP-activated protein kinase (AMPK) and suppressed the levels of sterol regulatory element-binding protein-1c (SREBP1c) and fatty acid synthase (FAS). Blockade of AMPK with the chemical inhibitor Compound C reversed the ability of OXT to suppress the SREBP1c/FAS axis and reduce lipid accumulation in hepatocytes. Additionally, OXT inhibited the nuclear translocation of SREBP1c in OA-treated cells. ***Conclusions:*** The findings demonstrate that OXT may serve as a potential therapeutic agent for MASLD by regulating the AMPK/SREBP1c/FAS pathway in lipid metabolism.

Citation of this article: Xu Y, Lu S, Wu H, Wu H, Li M, Zhou M, *et al*. Oxytocin Attenuates Metabolic Dysfunction-associated Steatotic Liver Disease via AMPK/SREBP1c/FAS-mediated Suppression of Hepatic Lipogenesis. J Clin Transl Hepatol 2025. doi: 10.14218/JCTH.2025.00213.

Introduction

With the global prevalence of sedentary lifestyles and Western dietary patterns, metabolic dysfunction-associated steatotic liver disease (MASLD) has emerged as the most common chronic hepatic disease. Epidemiological studies have reported an alarming prevalence of MASLD in both developed and developing countries, with rates of 25.3% in the United States and 29.2% in China.[1,2] MASLD is characterized by a spectrum of liver conditions, including simple steatosis, metabolic-associated steatohepatitis (MASH), fibrosis, cirrhosis, and hepatocellular carcinoma.[2] MASLD, evolving from the previous classification of nonalcoholic fatty liver disease (NAFLD), retains the same criteria for hepatic steatosis while requiring the presence of at least one cardiometabolic risk factor for diagnosis. Current evidence indicates negligible clinical discrepancies in these diagnostic entities, thereby validating the translational relevance of historical NAFLD research in the MASLD framework. Dietary control and exercise remain the primary interventive strategies for the treatment of MASLD.[3,4] However, their efficacy is mainly unsatisfactory due to the slow and arduous nature of these interventions. Therefore, effective pharmaceutical interventions may be highly beneficial for managing MASLD in the general population.[5,6]

Accumulating evidence indicates that lipid metabolism disorders, mitochondrial dysfunction, oxidative stress, and gut dysbiosis participate in the pathophysiology of MASLD.[7] Among them, abnormal lipid metabolism is a fundamental determinant of MASLD progression. Various pathological factors, such as tissue inflammation and circulating hormones, contribute to lipid metabolism and accumulation. Oxytocin (OXT) is a neuropeptide hormone secreted by neurocytes

Keywords: Oxytocin; Metabolic dysfunction-associated steatotic liver disease; MASLD; Lipid metabolism; AMP-activated protein kinase; AMPK signaling pathway.

[#]Contributed equally to this work.
[*]**Correspondence to:** Jinxia Liu, Department of Gastroenterology, Affiliated Hospital of Nantong University, Xisi Road, Nantong, Jiangsu 226001, China. ORCID: https://orcid.org/0000-0001-8327-2228. Tel: +86-13962946607, E-mail: liujinxia@ntu.edu.cn; Qin Jin, Department of Pathology, Affiliated Hospital of Nantong University, Xisi Road, Nantong, Jiangsu 226001, China. ORCID: https://orcid.org/0000-0002-7246-4651. Tel: +86-13626273670, E-mail: jinqin79@sina.com.

Copyright: © 2025 The Author(s). This article has been published under the terms of Creative Commons Attribution-Noncommercial 4.0 International License (CC BY-NC 4.0), which permits noncommercial unrestricted use, distribution, and reproduction in any medium, provided that the following statement is provided. "This article has been published in *Journal of Clinical and Translational Hepatology* at https://doi.org/10.14218/JCTH.2025.00213 and can also be viewed on the Journal's website at http://www.jcthnet.com".

in the hypothalamic paraventricular nucleus and supraoptic nucleus.[8] OXT stimulates uterine contractions, reduces postpartum hemorrhage, and promotes milk secretion. Additionally, OXT suppresses appetite, promotes energy metabolism, regulates peptide synthesis and secretion, and reduces inflammation.[8–11] Exogenous OXT has been shown to exert effects on body weight, lipid levels, and glucose homeostasis, highlighting its therapeutic potential for metabolic disorders. However, it is vital to clarify whether endogenous OXT participates in metabolic homeostasis. Recent research has identified OXT as an important regulator of adipose tissue lipolysis in both mice and humans.[12] Previous bioinformatics analyses have concentrated on the differential expression of OXT in 14 pairs of steatotic livers and healthy controls, demonstrating the role of OXT in MASLD progression.[13] Moreover, the oxytocin receptor (OXTR) is detectable in the liver and cultured hepatoma cell lines, including HepG2 and primary hepatocytes.[14,15] However, the diagnostic and therapeutic potential of the OXT-OXTR pathway in MASLD remains elusive.

In the present study, OXT expression levels and its related pathways in MASLD datasets were assessed. Reduced expression levels of OXT were found in MASLD patients, oleic acid (OA)-treated HepG2 cells, and high-fat diet (HFD)-fed mice. Experiments were conducted to investigate the molecular mechanisms by which exogenous OXT could regulate MASLD progression. The findings demonstrated a protective role of OXT in MASLD progression, which was mediated by the regulation of lipid metabolism through the AMP-activated protein kinase (AMPK) signaling pathway. The results demonstrated that OXT could exert a lipid metabolism-ameliorating effect on MASLD development, highlighting its potential preventive and therapeutic applications for MASLD management.

Methods

Acquisition and analysis of datasets

MASLD-related datasets were obtained from the Gene Expression Omnibus database(https://www.ncbi.nlm.nih.gov/geo/).[1] In the GSE126848 dataset, five non-alcoholic fatty liver (NAFL) male patients and 14 control subjects were selected, while abnormal samples were eliminated by cluster analysis. Samples from all groups were analyzed using a Venn diagram and principal component analysis. Genes from the two groups were analyzed using variance and ranked in descending order by $\log_2$FC. In addition, the heatmap was created using the "ComplexHeatmap" package based on the results of gene set enrichment analysis (GSEA). In the GSE48452 database, four NAFL patients and four MASH patients were selected. In the GSE53381 database, four standard diet-fed mice (hereinafter referred to as STD group) and four high-fat and high-cholesterol-fed mice (HFHC group) were chosen. In the GSE135251 dataset, 51 NAFL patients were selected. On the basis of median OXT gene expression level, these patients were classified into high- and low-risk groups. Differentially expressed genes were also sorted by $\log_2$FC. GSEA was performed for the OXT signaling pathway from the Kyoto Encyclopedia of Genes and Genomes and metabolism-related biological processes from Gene Ontology using the "ClusterProfiler" R package.[13] A p-value < 0.05 was considered statistically significant.

Reagents and antibodies

OXT for cellular experiments was obtained from Absin Bioscience (HPLC ≥ 95%, CAS 50-56-2, Shanghai, China). OXT for murine experiments was purchased from GenScript (purity ≥ 95%, Nanjing, China). Rabbit anti-OXT polyclonal antibody (pAb) and OA were purchased from Absin Bioscience (Shanghai, China). Anti-glyceraldehyde 3-phosphate dehydrogenase (GAPDH) mouse monoclonal antibody and anti-sterol regulatory element-binding protein-1c (SREBP1c) rabbit pAb were obtained from Servicebio (Wuhan, China). Anti-AMPK alpha 1 and phospho-AMPK alpha pAb antibodies were purchased from Proteintech (Wuhan, China). Anti-fatty acid synthase (FAS) rabbit pAb antibody was obtained from Wanleibio (Shenyang, China).

Patient samples and clinical data

The clinical data and serum samples of 113 MASLD patients and 63 healthy controls were collected from the Affiliated Hospital of Nantong University (Nantong, China) from September 2020 to December 2021. Liver tissues were obtained from three MASLD patients by liver biopsy and from three healthy controls by trauma surgery. Inclusion criteria were as follows: MASLD was diagnosed in a fasting state based on abdominal ultrasonography, which was performed by experienced and trained technicians. Diagnosis was evaluated using four ultrasonographic features: hepatorenal echo contrast, liver brightness, deep attenuation, and vascular blurring.[16] Hepatic steatosis severity was classified into three grades, with patients falling into grade I (mild) and grade II (moderate). Exclusion criteria were as follows: participants with a history of alcohol overconsumption over the past 12 months (>210 g per week for men, >140 g for women); those on steatogenic medications (e.g., amiodarone, methotrexate, tamoxifen, glucocorticoids), lipid-lowering drugs, antihypertensives, antibiotics, cortisol, oral contraceptives, or anti-inflammatory drugs; participants with viral, genetic, autoimmune, or drug-induced liver disease; and those with kidney, thyroid, gastrointestinal, or autoimmune diseases, polycystic ovary syndrome, or cancer were excluded.[17,18] Participants in the control group underwent a routine health screening program. Informed written consent was obtained from all participants, and the study protocol was approved by the Institutional Review Board of the Affiliated Hospital of Nantong University (Approval No. 2020-L097).

Cell culture

The HepG2 hepatoblastoma cell line was purchased from the Institute of Cell Biology, Chinese Academy of Sciences. The cell line was authenticated through STR profiling before being sent to us. HepG2 cells were exposed to 0.5 mM OA for 24 h to establish an *in vitro* steatosis model.[15] For OXT treatment, OA-treated HepG2 cells were further incubated with different concentrations (10^{-4}, 10^{-6}, and 10^{-8} M) of OXT for an additional 24 h.[15]

HepG2 cells were subjected to OA-induced steatosis (0.5 mM OA, 24 h), followed by treatment with 10^{-8} M OXT, with or without the addition of 10 μM Compound C (BML-275; MedChemExpress, Monmouth Junction, NJ, USA) for an additional 24 h. Compound C was added 1 h prior to OXT treatment and maintained throughout co-incubation. Cells were subsequently harvested for Western blot analysis.

Animal study

For this experiment, four-week-old male C57BL/6 mice (16–20 g) were purchased from the Laboratory Animal Center of Nantong University. All mice were maintained in standard isolator cages at 20 ± 2°C with a humidity of 50% ± 10% and under a 12 h/dark cycle. After two weeks of acclimation, mice were randomly assigned to four groups. Group 1: Mice were fed with a normal chow diet for 16 weeks and received

a saline intraperitoneal injection for four weeks (NCD group, n = 3). Group 2: Mice were fed with an HFD containing 45% fat (Double Lion Experimental Animal Feed Technology, Suzhou, China) for 16 weeks and received a saline intraperitoneal injection for four weeks (HFD group, n = 3). Group 3: Mice were fed with an HFD for 14 weeks and received OXT (50 nmol/d i.p.) intraperitoneal injection for two weeks (OXT 2W group, n = 4). Group 4: Mice were fed with an HFD for 16 weeks and received OXT (50 nmol/d i.p.) intraperitoneal injection for four weeks (OXT 4W group, n = 4).[19] Mice were weighed individually every week until the experimental endpoint. Liver and blood samples were collected for subsequent assays.

Biochemical analysis

Blood was obtained from the eyeballs of anesthetized animals and centrifuged at 3,000 rpm for 10 m at 4°C. Serum was collected and analyzed for measuring the levels of alanine transaminase (ALT), total cholesterol (TC), and low-density lipoprotein (LDL) cholesterol using a biochemical autoanalyzer (Fuji Medical System, Tokyo, Japan).

Western blotting

Tissue and cell samples were lysed with RIPA lysis buffer (P0013B, Beyotime) supplemented with 1× protease inhibitor cocktail (A32963, Thermo Fisher Scientific) and 1 mM phenylmethylsulfonyl fluoride using Dounce homogenizers. The lysates were incubated on ice for 30 m, followed by centrifugation at 13,000 g for 10 m at 4°C. The supernatant was transferred and subjected to the BCA protein assay (Thermo Fisher Scientific, Waltham, MA, USA). Equal amounts of protein samples were separated on 10% sodium dodecyl sulfate–polyacrylamide gel electrophoresis and then transferred onto polyvinylidene difluoride membranes (Bio-Rad, Hercules, CA, USA), followed by blocking with TBST containing 5% skim milk for 1.5 h. Thereafter, the membranes were incubated with primary antibodies at 4°C overnight and subsequently incubated with a secondary antibody for 2 h.[20] Protein bands were visualized by a bioimaging system (Bio-Rad) with an enhanced chemiluminescent kit (NCM Biotech, Suzhou, China). GAPDH was used as an internal control.

RNA extraction and reverse transcription quantitative polymerase chain reaction (PCR)

Total RNA samples were extracted using TRIzol reagent (Ambion, Austin, TX, USA) and reversely transcribed using the first-strand cDNA synthesis kit (Vazyme, Nanjing, China) following the manufacturer's instructions. The expression levels of target genes were quantified and analyzed using a SYBR Green PCR master mix (Qiagen, Hilden, Germany) on a Roche LightCycler 480 system (Roche Holding AG, Basel, Switzerland). 18S RNA was employed as an internal control.[21] Primer sequences were obtained from Sangon Biotech Co., Ltd. (Shanghai, China). The primers used for reverse transcription quantitative PCR are listed in Supplementary Table 1.

Enzyme-linked immunosorbent assay (hereinafter referred to as ELISA)

Serum concentration of OXT was measured using a Human OXT ELISA kit (Shanghai Fusheng Industrial Co., Ltd., Shanghai, China).

Oil Red O staining

Cells were first fixed with 4% paraformaldehyde for 30 m. Thereafter, cells were stained with a Modified Oil Red O Staining Kit (Beyotime Biotechnology, Shanghai, China) for 20 m in the dark. Cell samples were briefly washed using 60% isopropanol, rinsed with phosphate-buffered saline (PBS), and examined under an inverted microscope (magnification, 100×). Liver sections were stained with modified Oil Red O reagent for 10 m, washed with 60% ethanol, rinsed with distilled water, and dyed with hematoxylin for 90 s. The sections were sealed with 50% glycerol, followed by observation under a light microscope (magnification, 400×).[21] Two tissues with six non-overlapping fields were randomly selected from each group of animals to quantitatively analyze the degree of lipid accumulation using Fiji software.

Immunofluorescence

Frozen sections were immersed in blocking buffer for 30 m. Thereafter, sections were incubated with the primary antibody against OXT (Abcam, Cambridge, UK, 1:500) overnight at 4°C and fluorescein-conjugated secondary antibody (ABclonal Technology, Woburn, MA, USA) for 2 h at room temperature. Sections were sealed with mounting solution containing 5 μM DAPI for nuclear counterstain and examined under an inverted fluorescence microscope (magnification, 400×; Olympus, Tokyo, Japan). Cells growing on glass cover slides were rinsed with PBS once, fixed with 4% paraformaldehyde for 15 m, permeabilized with 0.2% Triton X-100 for 10 m, and blocked with 5% bovine serum albumin buffer at 4°C overnight. Subsequently, cells were incubated with an anti-SREBP1c antibody (Santa Cruz Biotechnology, Dallas, TX, USA; 1:50) for 12 h. After three washes, the slides were incubated with corresponding fluor-labeled secondary antibodies (ABclonal Technology), followed by nuclear staining with 5 μM DAPI. The slides were mounted and examined using a confocal laser-scanning microscope (LSM900; Zeiss, Oberkochen, Germany).[21]

Immunohistochemistry analysis

Paraffin-embedded tissue sections were dewaxed with xylene and then dehydrated using a gradient ethanol series, followed by antigen retrieval using EDTA buffer (pH 9.0). After blocking endogenous peroxidase activity using 3% hydrogen peroxide at room temperature for 15 m, the sections were blocked with blocking buffer (10% goat normal serum, 1% bovine serum albumin in PBS) and incubated with an anti-OXT primary antibody (1:6,000, Abcam). Subsequently, incubation was conducted using a secondary horseradish peroxidase-conjugated goat anti-rabbit IgG antibody (Zhongshan Jinqiao Biotechnology, Beijing, China). OXT immunoreactivity was visualized using a 3,3′-diaminobenzidine reagent (Dako, USA).[22] Finally, after sealing with neutral resin, all sections were observed under a light microscope (magnification, 100×; Leica) and quantitatively analyzed using Fiji software.

Hematoxylin and eosin (H&E) staining

H&E staining was performed to determine histopathological changes using a standard H&E staining protocol.[21] H&E-stained sections were independently and blindly evaluated by two experienced pathologists who were unaware of the clinical information and grouping. Steatosis was scored based on the percentage of hepatocytes containing lipid droplets as follows: 0 (<5%), 1 (5–33%), 2 (34–66%), 3 (>66%).[23]

MASLD activity score

Mouse liver sections were assessed by the MASLD activity score (NAS, 0–8), in terms of the combination of severity of steatosis (0–3), hepatocellular ballooning (0–2), and lobular

inflammation (0–3).[24] The stages of MASLD were classified based on the total NAS scores as follows: <3, not-MASH; ≥5, definite-MASH; 3–4, borderline-MASH.

Statistical analysis

Statistical analysis was conducted using GraphPad Prism 9 software (GraphPad Software Inc., San Diego, CA, USA). Continuous variables were expressed as mean ± standard deviation, while categorical variables were presented as frequency and percentage. An unpaired Student's t-test was used to make comparisons between two groups. For comparing multiple groups with a single factor, statistical analysis was performed using one-way analysis of variance followed by Dunnett's post hoc test. Binary logistic regression analysis generated odds ratios with 95% confidence intervals, adjusting for clinically relevant confounders, including age and gender. Stepwise multivariate logistic regression analysis was employed to identify independent predictors, with variables retained in the final model demonstrating statistical significance at $p < 0.05$. Significant differences were indicated as follows: ****$p < 0.0001$; ***$p < 0.001$; **$p < 0.01$; *$p < 0.05$; ns, not significant.

Results

OXT expression level in MASLD datasets

To decipher the role of OXT in MASLD progression, the expression level of OXT among non-NAFL, NAFL, and MASH subjects was evaluated. To this end, data of five NAFL patients and 14 healthy controls were obtained from the GSE126848 dataset (Fig. 1A). The principal component analysis indicated that the NAFL and control groups were remarkably separated (Fig. 1B). As shown in Figure 1C, OXT-associated pathways were significantly enriched in the control group compared with the NAFL group, as evidenced by GSEA (NES = −1.72, FDR = 0.005). In line with the GSEA results, OXT expression level was markedly downregulated in the NAFL group compared with the control group in the heatmap (Fig. 1D). Furthermore, OXT expression level was significantly reduced in the human MASH group (n = 4) compared with the NAFL group (n = 4, $p < 0.05$), implicating that OXT loss was positively correlated with the severity of hepatic steatosis (Fig. 1E). Furthermore, OXT expression level was significantly lower in HFHC mice (n = 4) than that in the STD group (n = 4) (Fig. 1F). Further GSEA of the GSE48452 dataset revealed significantly positive enrichment of the AMPK signaling pathway in the OXT high-expression cohort (Supplementary Fig. 1A). Key genes of this pathway exhibited clustered enrichment at the leading edge of the OXT-correlated gene ranking, as indicated by a prominent peak in the enrichment score curve. This provides robust bioinformatic support for our mechanistic concentration on the AMPK signaling pathway and its downstream lipogenic SREBP1c/FAS axis. These data explicitly indicate that OXT expression level was progressively reduced during MASLD development.

OXT downregulation was associated with worsened progression of MASLD

To validate the results obtained from publicly available data, the expression level of OXT in liver and serum samples of our cohort was assessed. As predicted, hepatic OXT expression level was significantly downregulated in MASLD patients compared with that in healthy controls (Fig. 2A). Furthermore, significantly decreased serum OXT level was identified in clinical MASLD patients in comparison with healthy controls (Fig. 2B).

The demographic data of MASLD patients and healthy controls are summarized in Supplementary Table 2. Body mass index (BMI), serum levels of gamma-glutamyl transferase, ALT, aspartate transaminase, TC, triglyceride (TG), and LDL were significantly higher in the MASLD group than those in the healthy control group. However, high-density lipoprotein level was significantly lower in the MASLD group than that in the healthy control group (Fig. 2C). After adjusting for age and sex, non-conditional logistic regression analysis indicated that weight, BMI, and serum levels of ALT, aspartate transaminase, TC, TG, high-density lipoprotein, LDL, glycosylated hemoglobin type A1c, and fasting blood glucose were significantly associated with an increased risk of MASLD (Supplementary Table 2, $p < 0.05$). However, no significant difference was noted in height or serum levels of gamma-glutamyl transferase, blood uric acid, blood urea nitrogen, and creatinine between the two groups. Stepwise logistic regression analysis demonstrated that BMI, ALT, TG, and OXT expression level served as independent indicators of MASLD progression (Table 1, $p = 0.025$).

To validate the relationship between OXT expression level and MASLD progression, liver tissues from 16 MASLD patients were analyzed across different steatosis grades and six healthy controls. H&E staining confirmed minimal lipid accumulation in control livers (score = 0), while MASLD patients exhibited progressive steatosis (Supplementary Fig. 1B). Immunohistochemistry revealed significantly attenuated OXT expression level (quantified by MOD) in the livers of MASLD patients compared with healthy controls (Supplementary Fig. 1B; $p < 0.01$). Representative cases from steatosis grades 1 (MASLD 1), grade 2 (MASLD 2), and grade 3 (MASLD 3) are illustrated in Supplementary Figure 1B. Crucially, correlation analysis revealed a significant negative correlation between hepatic steatosis scores and OXT expression level (Supplementary Fig. 1C; R = −0.9336, $p < 0.01$). These findings further solidify that decreased intrahepatic OXT expression level was closely associated with disease severity (steatosis) in clinical MASLD patients, positioning OXT as a potential biomarker for stratifying MASLD severity.

OXT ameliorated lipid accumulation in OA-treated HepG2 cells

Next, it was attempted to investigate whether OXT could participate in the regulation of lipid metabolism in hepatocytes. Using OA-exposed HepG2 cells as an *in vitro* steatosis model, it was revealed that OXT expression level was markedly reduced following hepatic steatosis (Fig. 3A and B, $p < 0.01$). Moreover, this study examined whether OXT treatment could influence hepatic lipid accumulation. HepG2 cells were exposed to different concentrations (10^{-4}, 10^{-6}, and 10^{-8} M) of OXT for 24 h according to previous studies.[15,19,20] Oil Red O staining indicated apparent accumulation of lipid droplets in OA-treated cells (Fig. 3C and D). Notably, when assessing the effect of OXT exposure on OA-induced lipid storage in HepG2 cells, OXT supplementation significantly attenuated lipid accumulation in OA-treated HepG2 cells (Fig. 3C). Of great intrigue, it was revealed that physiologically relevant OXT concentration (10^{-8} M) elicited a better effect in the amelioration of lipid accumulation than higher OXT concentrations (10^{-4} and 10^{-6} M), highlighting the therapeutic potential of low-dose OXT administration in MASLD management.[25,26]

OXT administration alleviated hepatic steatosis in MASLD mice

Furthermore, this study clarified whether OXT administration could ameliorate MASLD progression *in vivo*. A rodent MASLD model was successfully established with HFD feeding (Fig.

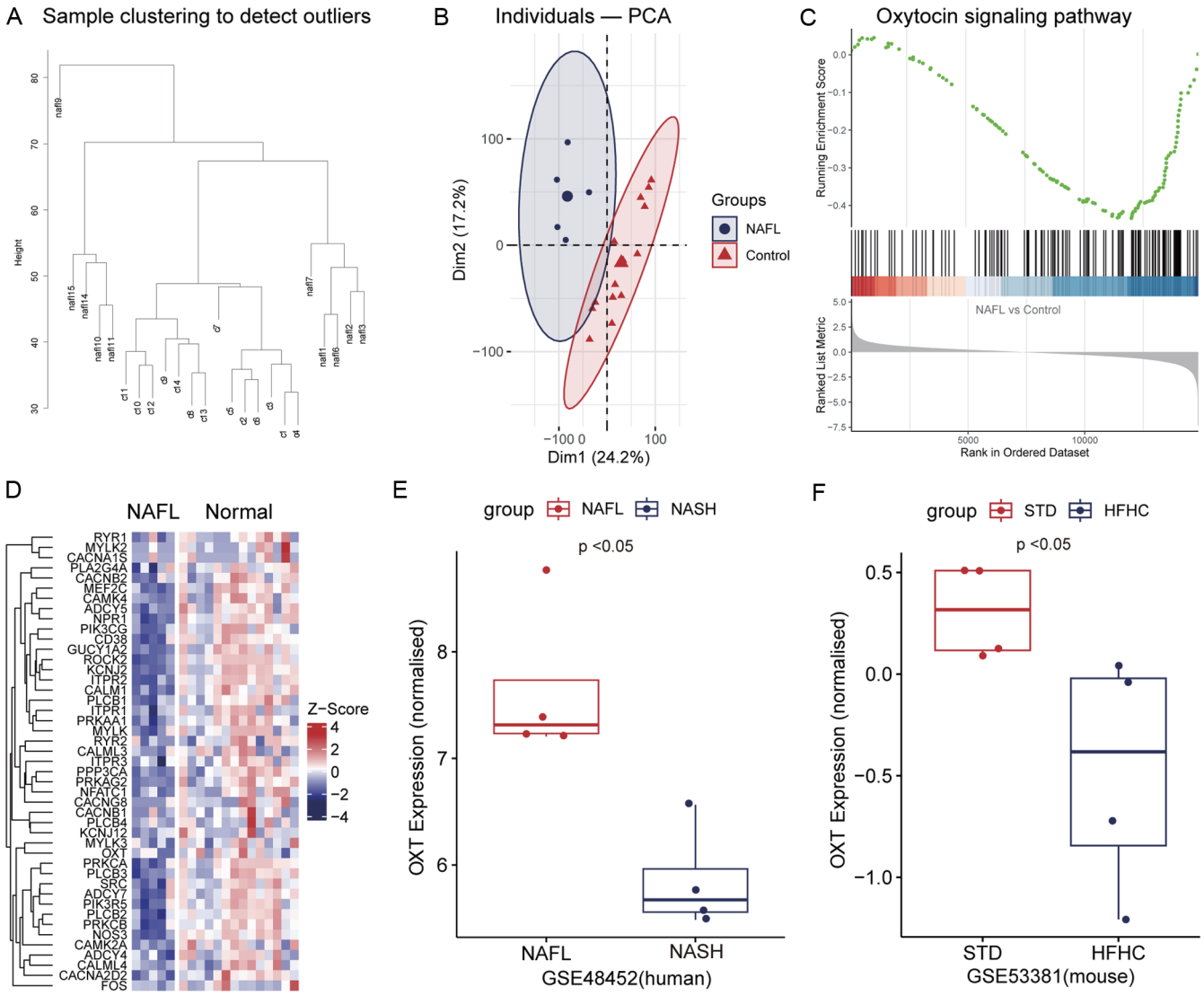

Fig. 1. Bioinformatics analysis of OXT expression levels in MASLD. (A) Sample clustering of NAFL patients and healthy controls from the publicly available GEO dataset GSE126848 (Control, n = 14; NAFL, n = 5). Abnormal samples were excluded through sample-level clustering analysis. (B) Principal component analysis (PCA) of the control and NAFL samples after removing the outlier. (C) Gene set enrichment analysis (GSEA) of the OXT signaling pathway using the KEGG database. (D) Heatmap of genes involved in the OXT signaling pathway between the control group and the NAFL group. OXT was highlighted in red. (E) Comparison of serum OXT levels between the NAFL group and the MASH group in male subjects from the GSE552 dataset (NAFL, n = 4; MASH, n = 4). (F) Comparison of serum OXT levels between STD- and HFHC-fed mice in the GSE53381 dataset (STD, n = 4; HFHC, n = 4). $p < 0.05$ was considered statistically significant. MASLD, metabolic dysfunction-associated steatotic liver disease; NAFL, non-alcoholic fatty liver; GEO, gene expression omnibus; GSEA, Gene set enrichment analysis; KEGG, kyoto encyclopedia of genes and genomes; MASH, metabolic-associated steatohepatitis; STD, standard diet; HFHC, high fat high cholesterol; OXT, oxytocin.

4A). Beginning at week 12 of HFD feeding, mice received either vehicle control or OXT (50 nmol/kg/day) for two or four weeks, at a dose previously reported in the literature.[27] OXT expression level was significantly reduced in the HFD group compared with the NCD group (Fig. 4B, $p < 0.01$). Average body weight was significantly elevated in the HFD group after 12 weeks of feeding compared with the NCD group. However, OXT treatment resulted in notable weight loss in the OXT 2W and OXT 4W groups compared with the HFD group (Fig. 4C). Notably, OXT administration significantly reduced serum levels of ALT, TC, and LDL cholesterol in HFD-fed animals (Fig. 4D). With exogenous OXT injection, OXT expression level in the livers of the HFD-fed group was restored to a level comparable with the NCD group, as revealed by immunohistochemistry staining (Fig. 4E). H&E and Oil Red O staining indicated that OXT supplementation significantly diminished lipid accumulation in HFD mice (Fig. 4E). NAS score further confirmed that OXT intervention significantly alleviated the severity of MASLD (Fig. 4F). Collectively, these findings provided solid evidence that OXT administration could mitigate hepatic lipid accumulation and MASLD progression in the experimental animal model.

OXT inhibited lipogenesis via the AMPK signaling pathway

Bioinformatics analysis of human MASLD datasets indicated that OXT was potentially involved in fatty acid metabolism (Fig. 5A). The mRNA levels of SREBP1c, FAS, ATP citrate

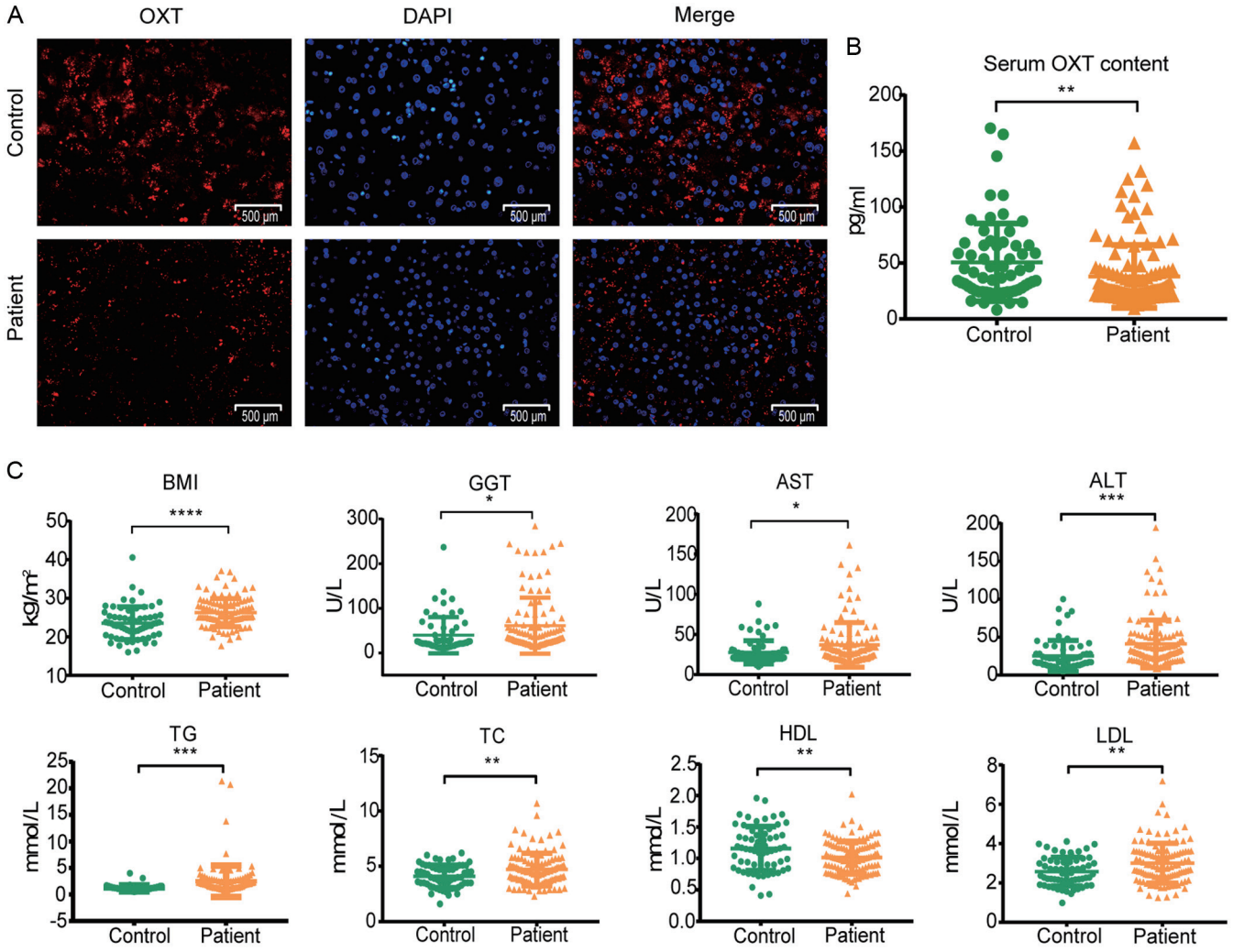

Fig. 2. Expression levels of OXT in MASLD patients. (A) Immunofluorescence staining of OXT (red) in liver tissues of MASLD patients and healthy controls (magnification, 400×). (B) ELISA of serum levels of OXT in MASLD patients and healthy controls. (C) Serum levels of BMI, GGT, AST, ALT, TG, TC, HDL-C, and LDL-C in MASLD patients (n = 113) and healthy controls (n = 63). ****$p < 0.0001$; ***$p < 0.001$; **$p < 0.01$; *$p < 0.05$. MASLD, metabolic dysfunction-associated steatotic liver disease; ELISA, enzyme linked immunosorbent assay; BMI, body mass index; GGT, serum levels of glutamyl transferase; AST, aspartate transaminase; ALT, alanine aminotransferase; TG, triglyceride; TC, total cholesterol; HDL-C, high-density lipoprotein cholesterol; LDL-C, low-density lipoprotein cholesterol; OXT, oxytocin.

lyase (ACLY), acetyl-CoA carboxylase (ACC) 1, stearoyl-CoA desaturase (SCD) 1, liver X receptor alpha, and CD36 were significantly downregulated following OXT treatment in OA groups (Fig. 5B). Of note, SREBP1c, a key transcription factor of lipogenic gene induction, exhibited the most significant reduction among all genes examined. Notably, the nuclear translocation of SREBP1c was inhibited by OXT supplementation in OA-treated cells (Fig. 5C). Furthermore, OXT treatment significantly increased the phosphorylated AMPK (p-AMPK)/total-AMPK ratio and decreased the overall expression levels of SREBP1c and FAS in OA-treated cells (Fig. 5D). Consistently, it was revealed that the expression levels of p-AMPK, SREBP1c, and FAS followed the same trend in the livers of the OXT-administered animal model (Fig. 5E). Moreover, animals receiving OXT supplementation for four weeks exhibited higher molecular alterations than those with two-week OXT administration.

Table 1. Multivariate analysis of independent factors for the relationship of MASLD

Factors	Odds ratio (95% CI)	*P*-value
BMI	1.145 (1.027–1.276)	0.015
ALT	1.025 (1.007–1.043)	0.006
TG	4.923 (2.296–10.553)	<0.001
Oxytocin	0.986 (0.974–0.998)	0.025

Variables of FBG and HbA1c were excluded from the final stepwise logistic regression analysis for high incidence of missing data (42/176, 98/176, respectively). MASLD, metabolic dysfunction-associated steatotic liver disease; BMI, body mass index; ALT, alanine aminotransferase; TG, triglyceride.

To validate the causal role of AMPK activation in OXT's protective effects, the specific AMPK inhibitor Compound C was employed to assess its impact on the OXT-initiated AMPK/SREBP1c/FAS signaling axis. As displayed in Supplementary Figure 1D, Western blot analysis revealed that Compound C treatment significantly attenuated OXT-induced AMPK phosphorylation (p-AMPK/GAPDH ratio), and SREBP1c and FAS downregulation compared with the OA + OXT group. These

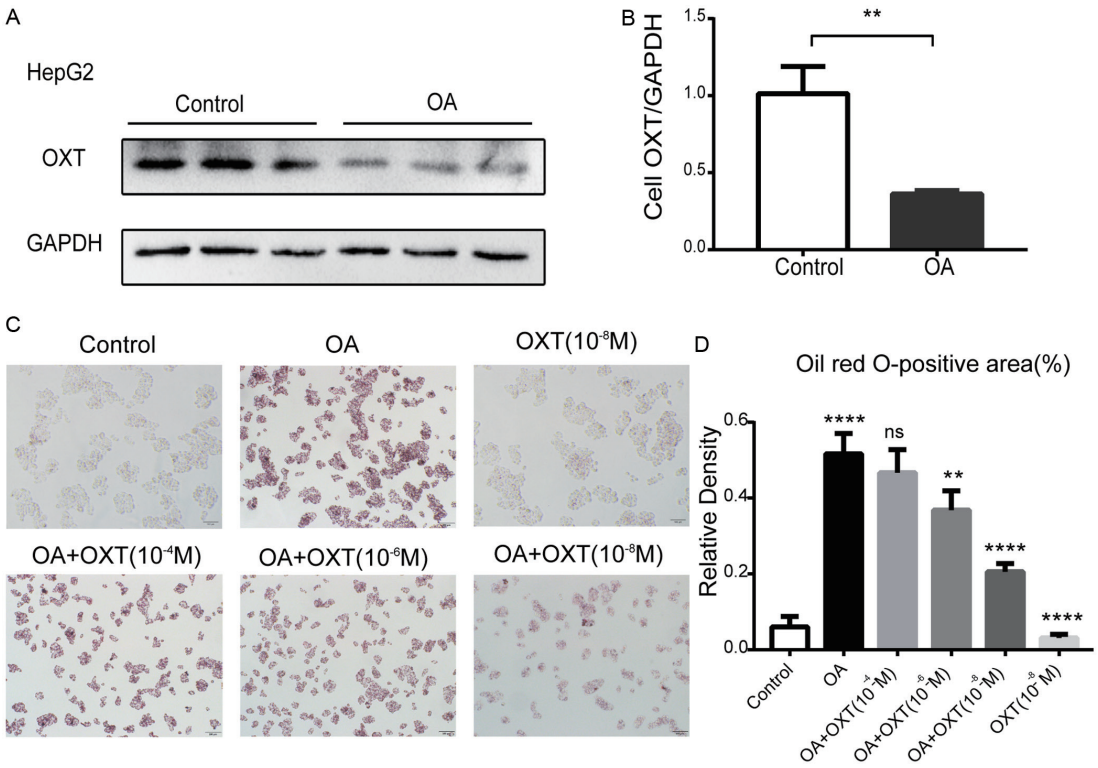

Fig. 3. The effects of OXT on lipid accumulation in OA-treated HepG2 cells. (A) Western blot analysis of OXT expression levels in OA-exposed HepG2 cells. (B) Quantitative analysis of OXT expression levels in OA-exposed HepG2 cells. (C) Representative images of Oil Red O staining of HepG2 cells with or without OXT treatment (magnification, 100×). HepG2 cells were incubated with OA for 24 h. Three concentrations (10^{-4}, 10^{-6}, and 10^{-8} M) of exogenous OXT were given to OA-treated HepG2 cells for 24 h. (D) Quantitative analysis of Oil Red O staining of cells across all groups. ****$p < 0.0001$; **$p < 0.01$; ns, no significance. OA, oleic acid; GAPDH, Glyceraldehyde 3-phosphate dehydrogenase; OXT, oxytocin.

results demonstrated that AMPK activation was critically required for OXT to suppress the SREBP1c/FAS signaling axis and mitigate lipid accumulation in hepatocytes. Collectively, these results revealed that OXT ameliorated MASLD through activation of the AMPK signaling pathway.

Discussion

MASLD is one of the most common metabolic disorders and is closely associated with the epidemic of obesity and type 2 diabetes mellitus.[28] It encompasses a wide spectrum of pathological changes, ranging from simple steatosis to steatohepatitis, fibrosis, and eventually advanced cirrhosis.[29] Early intervention is crucial for preventing the progression of MASLD.[21] However, there are few available interventions, and no pharmacological agents have been broadly adopted in clinical practice for this severe chronic condition.[30]

Data obtained from public datasets and our cohort both revealed that OXT expression level was negatively correlated with MASLD progression. Notably, stepwise logistic regression analysis of clinical data indicated that OXT was an independent prognostic factor of MASLD. This is consistent with previous studies, demonstrating that OXT downregulation is a critical event and diagnostic biomarker of steatosis.[13] However, whether OXT directly participates in metabolic control during the development of MASLD remains elusive. A recent study demonstrated that administration of long half-life OXT peptide analogs at nmol/kg doses exerted dose-dependent antidiabetic and anti-obesity effects on rodents, highlighting a beneficial influence of OXT in preventing metabolic disorders.[31] The dosage for OXT intraperitoneal injection in mice was determined based on relevant literature, which indicated a significant reduction in fatty liver under this dose range (10^{-8}–10^{-6} M).[19,27] Consistently, results of the present study also showed that intraperitoneal injection of OXT (50 nmol/d, i.p.) significantly reduced fatty liver in mice. Hence, it can be preliminarily concluded that the concentrations of OXT (10^{-6} M and 10^{-8} M) are appropriate for further studies. Nanomolar concentrations of OXT treatment also directly stimulate insulin and glucagon secretion from primary islets and induce lipolysis, PGE2, and leptin secretion from 3T3-L1 adipocytes.[9] These findings are consistent with our data, suggesting that nanomolar concentrations of OXT exposure can improve hepatic lipid and glucose metabolism *in vivo* and *in vitro*, highlighting a strong potential for using this dosage of OXT for interventive approaches in the treatment of MASLD.

Serving as a hypothalamic hormone, OXT has been reported to be involved in various physiological processes and pathological conditions. Various roles of OXT in the liver have been revealed through investigations conducted over the past decades. OXT can promote weight loss without causing excessive muscle and bone loss.[26] OXT has been shown to ameliorate hepatocyte injury following experimental renal ischemia-reperfusion.[23] Recent research has indicated that OXT could alleviate liver fibrosis through liver macrophages.[22] Additionally, OXT administration has been demonstrated to elevate glucagon levels in both normal and streptozotocin-induced diabetic rats.[32] Studies have revealed that OXTR is present in various metabolism-associated tissues, including the pancreas and the liver, where it is specifically

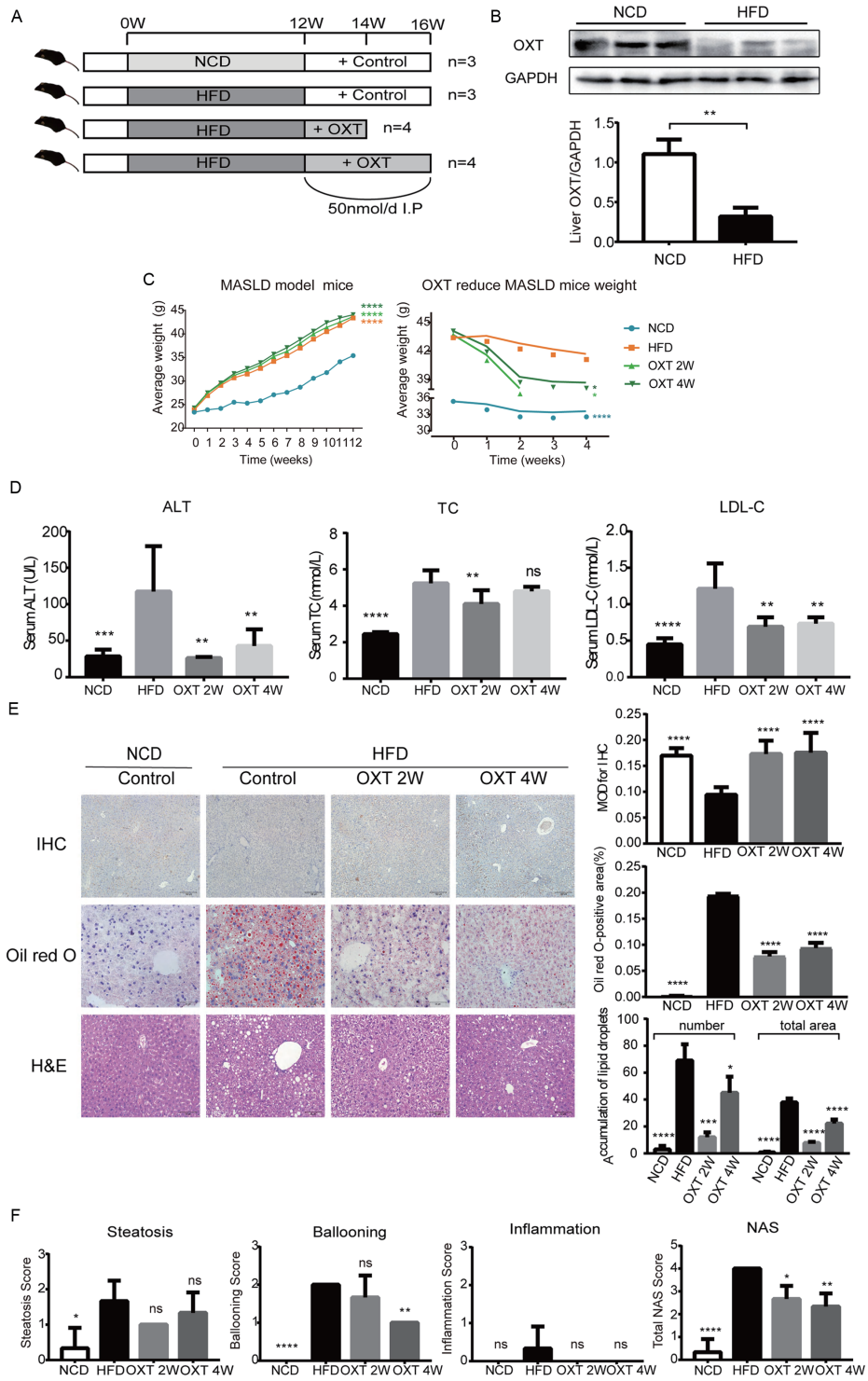

Fig. 4. The effects of OXT on hepatic steatosis in HFD-fed mice. (A) Schematic diagram of the experimental procedure of the HFD-fed mouse model. Mice were fed with HFD or NCD for 12 weeks. From week 13, the NCD group received daily intraperitoneal saline injections for four weeks (n = 3). HFD-fed mice were divided into three groups and received intraperitoneal injections daily as follows: HFD group, saline for four weeks, n = 3; OXT 2W group, OXT 50 nmol for two weeks, n = 4; OXT 4W group, OXT 50 nmol for four weeks, n = 4. (B) Western blot analysis of hepatic OXT expression levels in the indicated groups of mice. Statistical analysis of the OXT expression levels is shown below. (C) Average body weight of mice after 12 weeks of NCD or HFD feeding (left) and following saline or OXT treatment for two to four weeks (right). (D) Serum levels of ALT, TC, and LDL-C from the indicated groups. (E) Representative images of IHC, Oil Red O, and H&E staining of liver tissue sections. Quantitative analyses of staining are shown on the right. (F) Comparison of MASLD activity score (NAS) across all groups. ****$p < 0.0001$; ***$p < 0.001$; **$p < 0.01$; *$p < 0.05$; ns, no significance. MASLD, metabolic dysfunction-associated steatotic liver disease; HFD, high fat diet; NCD, normal chow diet; ALT, alanine transaminase; TC, total cholesterol; and LDL-C, low-density lipoprotein cholesterol; IHC, immunohistochemistry; H&E, hematoxylin and eosin; OXT, oxytocin.

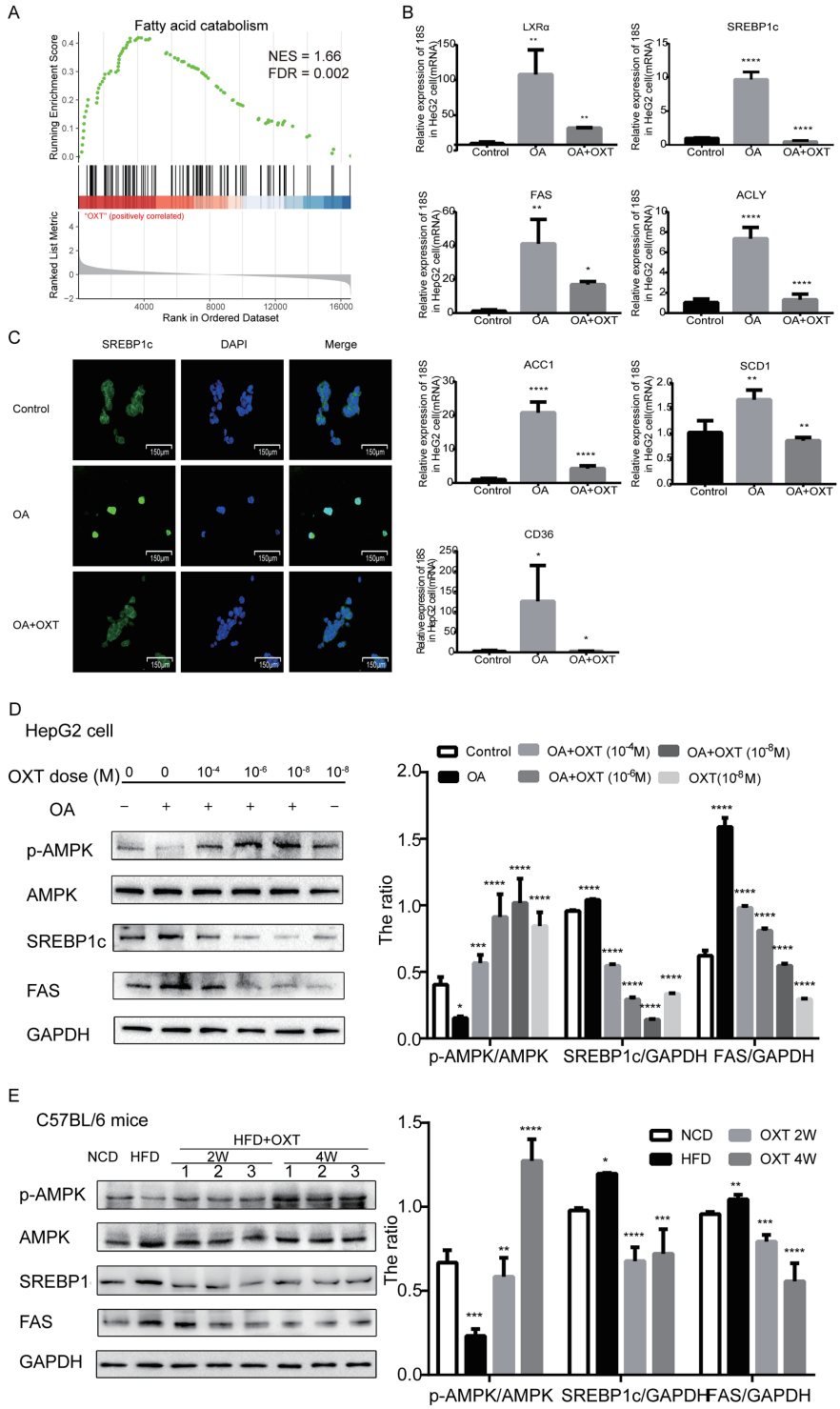

Fig. 5. OXT regulates lipid metabolism via the AMPK signaling pathway. (A) GSEA of OXT expression levels in the regulation of fatty acid metabolism in the MASLD dataset. (B) RT-PCR analysis of the mRNA expression levels of LXRα, SREBP1c, FAS, ACLY, ACC1, SCD1, and CD36. Data are presented as mean ± SD of three independent experiments. (C) Immunofluorescence analysis of the cellular localization of SREBP1c in the indicated groups of cells (200×). (D) The protein levels of p-AMPK, AMPK, SREBP1c, and FAS in OA- and OXT-exposed HepG2 cells were examined by Western blot analysis. (E) Western blot analysis of the protein expression levels of p-AMPK, AMPK, SREBP1c, and FAS in liver tissues of C57BL/6 mice. ****$p < 0.0001$; ***$p < 0.001$; **$p < 0.01$; *$p < 0.05$. AMPK, AMP-activated protein kinase; GSEA, gene set enrichment analysis; RT-PCR, reverse transcription quantitative real-time polymerase chain reaction; LXRα, liver X receptor alpha; SREBP1c, sterol regulatory element-binding protein-1c; FAS, fatty acid synthase; ACLY, ATP citrate lyase; ACC1, acetyl coenzyme A carboxylase alpha; SCD1, stearoyl-CoA desaturase 1; CD36, AMPK, AMP-activated protein kinase; p-AMPK, Phosphorylated AMP-activated Protein Kinase; SREBP1c, sterol regulatory element-binding protein-1c; FAS, fatty acid synthase; GAPDH, Glyceraldehyde 3-phosphate dehydrogenase; OXT, oxytocin; MASLD, metabolic dysfunction-associated steatotic liver disease; +, with; -, without.

expressed in hepatocytes.[33,34] In the pancreatic islets, OXTR protein has been exclusively found in both islet α and β cells. Therefore, it can be speculated that OXT may directly regulate liver metabolism via the hepatocyte OXTR pathway.

Accumulating evidence demonstrates that, in addition to its well-established roles in promoting parturition and lactation, OXT also plays significant metabolic roles in both sexes.[35] It has been previously reported that OXT can improve fatty liver, which impairs glucose and lipid metabolism, thereby promoting type 2 diabetes, metabolic syndrome, and cardiovascular disease, as well as increasing the risk of cirrhosis and liver cancer.[36] Studies have revealed that OXT partially counteracts the inactivation of glycogen synthase in the presence of insulin. The current study demonstrated that OXT supplementation reduced body weight, blood lipid levels, and liver injury in HFD-fed mice. OXT treatment also significantly decreased intracellular lipid accumulation and hepatic steatosis in OA-treated HepG2 cells. These results highlight a potential role of OXT administration in ameliorating lipid metabolism and NAFLD progression, confirming the merit of OXT-based therapies for metabolic disorders. Previous research has indicated that OXT-induced weight loss may be partly attributed to increased energy expenditure and/or lipolysis.[37] Moreover, OXT enhanced lipolysis in 3T3-L1 differentiated adipocytes by increasing autocrine/paracrine actions of prostaglandin and leptin.[9] OXT signaling restricts food ingestion in both human and animal models.[38] Intranasal OXT exerted a notable inhibitory impact on appetite in young men, especially for sweets.[39] In male rats, central OXT signaling inhibited the activity of ventral tegmental area dopamine neurons induced by food cues and modulated behaviors motivated by the reward of palatable foods.[40] Additionally, OXT administration in the hypothalamus could promote short-term energy intake and spontaneous physical activity.[41] Furthermore, OXT contributes to the ability of β-adrenergic agonists to adequately promote lipolysis. OXT from the peripheral nervous system is an endogenous regulator of fat and systemic metabolism.[12] OXT improved insulin sensitivity and glucose tolerance in HFD-fed rats after a 14-day infusion.[19] The bioinformatics analysis also demonstrated that OXT could potentially change fatty acid metabolism in the human GSE135251 dataset. This study employed GSEA and found significant enrichments in the fatty acid metabolism pathways in the high OXT expression group (Fig. 5A). According to the literature, fatty acid synthesis can be disrupted by the AMPK-SREBP1c signaling pathway. Phosphorylation of ACC1 and SREBP1c by AMPK reduces the activity of these key enzymes involved in lipid synthesis, leading to a significant reduction in hepatic lipid accumulation. Collectively, the present study, for the first time, indicated that OXT played an effective role in the treatment of MASLD both *in vitro* and *in vivo* by regulating lipid metabolism.

Notably, this study revealed that OXT administration downregulated mRNA expression levels of liver X receptor alpha, ACLY, ACC1, SREBP1c, FAS, SCD1, CD36, and especially SREBP1c. SREBP1c is an isoform of the SREBP family and serves as a master transcription factor that activates lipogenic genes, leading to hepatic lipid accumulation, insulin resistance, and dyslipidemia.[42] SREBP1c activation directly upregulates the expression levels of its downstream target molecules, including ACC1, ACLY, FAS, and SCD. The nuclear translocation of SREBP1c indicates its activation and maturity, promoting lipid uptake, as well as triglyceride and cholesterol synthesis through binding to sterol regulatory elements.[41] Moreover, this nuclear translocation increases lipid accumulation and accelerates the development of MASLD-related hepatocellular carcinoma.[43] In the present study, SREBP1c was translocated from the cytoplasm to the nucleus following OA exposure in HepG2 cells, which could be reversed by OXT intervention. Here, SREBP1c was considered one of the most important target genes modulated by OXT in MASLD progression.

Previous research revealed that SREBP1c was negatively correlated with the AMPK signaling pathway.[44] AMPK is considered a promising therapeutic target in metabolic disorders because of its positive effects on cytoprotective properties under circumstances of inflammation, oxidative stress, and endoplasmic reticulum stress.[45] AMPK mediates suppression of the mTOR/SREBP1 signaling pathway and phosphorylates ACC1 and ACC2 to regulate intracellular lipid metabolism.[46] Its activation suppresses steatosis and inflammation in the livers of obese mice.[47] In the present study, OXT treatment significantly increased the p-AMPK/total-AMPK ratio and decreased the overall expression levels of SREBP1c and FAS in OA-treated cells. Previous research has shown that the OXT signaling system activated downstream effectors such as NR4A1 via OXTR-mediated calcium influx, functioning as a phenotypic switch.[22] Moreover, calcium influx has been well documented to activate AMPK and lipid metabolic pathways to alleviate liver steatosis.[48] Because OXTR is detectable in various metabolism-associated tissues, including the liver, pancreatic islets, and adipose tissues,[3,4,33,34] it was hypothesized that OXT could exert its effects on the AMPK signaling pathway through OXTR activation and calcium influx.

Before considering OXT as a therapeutic agent for NAFLD, it is essential to assess its safety in adults, particularly regarding its long-term administration. Clinical trials have demonstrated that OXT is generally safe for prolonged use in patients with NAFLD, with no evidence of drug resistance. In one study, participants used three sprays per nostril (24 IU) four times daily (20–30 m before meals and at bedtime) for eight weeks.[49] The safety data were reassuring, indicating no serious adverse events between those receiving OXT and those receiving a placebo, although there were more reports of nasal irritation with OXT. In this clinical trial, subjects were randomized to receive intranasal OXT (40 USP units/mL, 4 IU/spray), and the trial results indicated that intranasal OXT has minimal adverse effects in patients.[50]

However, the limitations of this study should be pointed out. Despite involving more than one hundred subjects, the clinical data were collected from a single center. Future research will expand MASLD clinical data to large-scale multicenter studies across various regions. In addition, primary hepatocytes and OXT knockout mice employed for *in vitro* and *in vivo* experiments might provide better assessments for OXT treatment in MASLD. While the findings strongly demonstrate OXTR-mediated mechanisms, future studies employing tissue-specific OXTR knockout models will be essential to conclusively establish receptor specificity and exclude potential off-target effects. These investigations will serve as the foundation for ongoing research. OXT is a potential predictive marker and a novel therapeutic agent for MASLD. Future clinical use of OXT should address potential issues such as resistance to long-term use and the possibility of multisystem effects, particularly when administering OXT to children and adolescents.

Conclusions

The present study demonstrates that OXT treatment ameliorates lipid accumulation and accelerates lipid metabolism by regulating the AMPK/SREBP1c/FAS axis in MASLD progression. OXT is a potential indicator of disease progression and a

promising therapeutic agent for MASLD. The findings provide a new direction for the potential clinical applications of OXT.

Funding

This study was supported by the National Natural Science Foundation of China (Grant Nos. 82570690, 82272624, 8140 1985, and 31801113), the China Postdoctoral Science Foundation (Grant Nos. 2018M632830, 2020M670039ZX, and 2021M701793), the Natural Science Foundation of Jiangsu Province (Grant No. BK20211105), the Social Development Foundation of Nantong City (Grant Nos. MS12021073, MS22 022005, JCZ21061, JCZ20004, and MS22022014), the Jiangsu Provincial Research Hospital (Grant No. YJXYY202204), and the Nantong University School of Medicine Graduate Practice Innovation Program (Grant No. YJS2004040).

Conflict of interest

The authors have no conflict of interests related to this publication.

Author contributions

Study conception and design, data analysis and interpretation, writing of the manuscript (YX, SL), data generation and collection (YX, SL, HongW, HaiW, ML, MZ, TC, XW, LQ), revision of the manuscript (HaiW, ML, MZ, TC, XW, LQ, QJ, JL), and study supervision (QJ, JL). All authors read and approved the submitted version of the manuscript.

Ethical statement

All animal experiments were approved by the Institutional Animal Care and Use Committee at Nantong University (Approval No. S20210220-014), and were performed in compliance with the animal welfare guidelines of Nantong University. All animals received human care. Informed written consent was obtained from all participants in the study, and the ethical principle was approved by the Institutional Review Board of the Affiliated Hospital of Nantong University (Approval No. 2020-L097), in accordance with the Declaration of Helsinki (as revised in 2024).

Data sharing statement

The datasets used and analyzed during the present study are available from the corresponding author on reasonable request.

References

[1] Zhou J, Zhou F, Wang W, Zhang XJ, Ji YX, Zhang P, *et al*. Epidemiological Features of NAFLD From 1999 to 2018 in China. Hepatology 2020;71(5):1851–1864. doi:10.1002/hep.31150, PMID:32012320.
[2] Noureddin M, Ntanios F, Malhotra D, Hoover K, Emir B, McLeod E, *et al*. Predicting NAFLD prevalence in the United States using National Health and Nutrition Examination Survey 2017-2018 transient elastography data and application of machine learning. Hepatol Commun 2022;6(7):1537–1548. doi:10.1002/hep4.1935, PMID:35365931.
[3] Pouwels S, Sakran N, Graham Y, Leal A, Pintar T, Yang W, *et al*. Non-alcoholic fatty liver disease (NAFLD): a review of pathophysiology, clinical management and effects of weight loss. BMC Endocr Disord 2022;22(1):63. doi:10.1186/s12902-022-00980-1, PMID:35287643.
[4] Berná G, Romero-Gomez M. The role of nutrition in non-alcoholic fatty liver disease: Pathophysiology and management. Liver Int 2020;40(Suppl 1):102–108. doi:10.1111/liv.14360, PMID:32077594.
[5] Friedman SL, Neuschwander-Tetri BA, Rinella M, Sanyal AJ. Mechanisms of NAFLD development and therapeutic strategies. Nat Med 2018;24(7):908–922. doi:10.1038/s41591-018-0104-9, PMID:29967350.
[6] Raza S, Rajak S, Upadhyay A, Tewari A, Anthony Sinha R. Current treatment paradigms and emerging therapies for NAFLD/NASH. Front Biosci (Landmark Ed) 2021;26(2):206–237. doi:10.2741/4892, PMID:33049668.
[7] Tilg H, Adolph TE, Dudek M, Knolle P. Non-alcoholic fatty liver disease: the interplay between metabolism, microbes and immunity. Nat Metab 2021;3(12):1596–1607. doi:10.1038/s42255-021-00501-9, PMID:34931 080.
[8] Kerem L, Lawson EA. The Effects of Oxytocin on Appetite Regulation, Food Intake and Metabolism in Humans. Int J Mol Sci 2021;22(14):7737. doi:10.3390/ijms22147737, PMID:34299356.
[9] Assinder SJ, Boumelhem BB. Oxytocin stimulates lipolysis, prostaglandin E(2) synthesis, and leptin secretion in 3T3-L1 adipocytes. Mol Cell Endocrinol 2021;534:111381. doi:10.1016/j.mce.2021.111381, PMID:342 16640.
[10] Olszewski PK, Klockars A, Levine AS. Oxytocin: A Conditional Anorexigen whose Effects on Appetite Depend on the Physiological, Behavioural and Social Contexts. J Neuroendocrinol 2016;28(4). doi:10.1111/jne.12376, PMID:26918919.
[11] Yuan J, Zhang R, Wu R, Gu Y, Lu Y. The effects of oxytocin to rectify metabolic dysfunction in obese mice are associated with increased thermogenesis. Mol Cell Endocrinol 2020;514:110903. doi:10.1016/j.mce.2020.110903, PMID:32531419.
[12] Li E, Wang L, Wang D, Chi J, Lin Z, Smith GI, *et al*. Control of lipolysis by a population of oxytocinergic sympathetic neurons. Nature 2024;625(7993):175–180. doi:10.1038/s41586-023-06830-x, PMID:380 93006.
[13] Rezaei Tavirani M, Rezaei Tavirani M, Zamanian Azodi M. ANXA2, PRKCE, and OXT are critical differentially genes in Nonalcoholic fatty liver disease. Gastroenterol Hepatol Bed Bench 2019;12(2):131–137. PMID:31191837.
[14] Kusui C, Kimura T, Ogita K, Nakamura H, Matsumura Y, Koyama M, *et al*. DNA methylation of the human oxytocin receptor gene promoter regulates tissue-specific gene suppression. Biochem Biophys Res Commun 2001;289(3):681–686. doi:10.1006/bbrc.2001.6024, PMID:11726201.
[15] Luo D, Jin B, Zhai X, Li J, Liu C, Guo W, *et al*. Oxytocin promotes hepatic regeneration in elderly mice. iScience 2021;24(2):102125. doi:10.1016/j.isci.2021.102125, PMID:33659883.
[16] Hamaguchi M, Kojima T, Itoh Y, Harano Y, Fujii K, Nakajima T, *et al*. The severity of ultrasonographic findings in nonalcoholic fatty liver disease reflects the metabolic syndrome and visceral fat accumulation. Am J Gastroenterol 2007;102(12):2708–2715. doi:10.1111/j.1572-0241.2007.01526.x, PMID:17894848.
[17] Fan JG, Xu XY, Yang RX, Nan YM, Wei L, Jia JD, *et al*. Guideline for the Prevention and Treatment of Metabolic Dysfunction-associated Fatty Liver Disease (Version 2024). J Clin Transl Hepatol 2024;12(11):955–974. doi:10.14218/JCTH.2024.00311, PMID:39544247.
[18] Rooholahzadegan F, Arefhosseini S, Tutunchi H, Badali T, Khoshbaten M, Ebrahimi-Mameghani M. The effect of DASH diet on glycemic response, meta-inflammation and serum LPS in obese patients with NAFLD: a double-blind controlled randomized clinical trial. Nutr Metab (Lond) 2023;20(1):11. doi:10.1186/s12986-023-00733-4, PMID:36788518.
[19] Deblon N, Veyrat-Durebex C, Bourgoin L, Caillon A, Bussier AL, Petrosino S, *et al*. Mechanisms of the anti-obesity effects of oxytocin in diet-induced obese rats. PLoS One 2011;6(9):e25565. doi:10.1371/journal.pone.0025565, PMID:21980491.
[20] Morishima M, Tahara S, Wang Y, Ono K. Oxytocin Downregulates the Ca(V)1.2 L-Type Ca(2+) Channel via Gi/cAMP/PKA/CREB Signaling Pathway in Cardiomyocytes. Membranes (Basel) 2021;11(4):234. doi:10.3390/membranes11040234, PMID:33806201.
[21] Liu J, Yuan Y, Gong X, Zhang L, Zhou Q, Wu S, *et al*. Baicalin and its nanoliposomes ameliorates nonalcoholic fatty liver disease via suppression of TLR4 signaling cascade in mice. Int Immunopharmacol 2020;80:106208. doi:10.1016/j.intimp.2020.106208, PMID:31955065.
[22] Zhai X, Zhang H, Xia Z, Liu M, Du G, Jiang Z, *et al*. Oxytocin alleviates liver fibrosis via hepatic macrophages. JHEP Rep 2024;6(6):101032. doi:10.1016/j.jhepr.2024.101032, PMID:38882603.
[23] Tas Hekimoglu A, Toprak G, Akkoc H, Evliyaoglu O, Ozekinci S, Kelle I. Oxytocin ameliorates remote liver injury induced by renal ischemia-reperfusion in rats. Korean J Physiol Pharmacol 2013;17(2):169–173. doi:10.4196/kjpp.2013.17.2.169, PMID:23626480.
[24] Kleiner DE, Brunt EM, Van Natta M, Behling C, Contos MJ, Cummings OW, *et al*. Design and validation of a histological scoring system for nonalcoholic fatty liver disease. Hepatology 2005;41(6):1313–1321. doi:10.1002/hep.20701, PMID:15915461.
[25] Uvnäs-Moberg K, Ekström-Bergström A, Berg M, Buckley S, Pajalic Z, Hadjigeorgiou E, *et al*. Maternal plasma levels of oxytocin during physiological childbirth - a systematic review with implications for uterine contractions and central actions of oxytocin. BMC Pregnancy Childbirth 2019;19(1):285. doi:10.1186/s12884-019-2365-9, PMID:31399062.
[26] McCormack SE, Blevins JE, Lawson EA. Metabolic Effects of Oxytocin. Endocr Rev 2020;41(2):121–145. doi:10.1210/endrev/bnz012, PMID:31803919.
[27] Altirriba J, Poher AL, Caillon A, Arsenijevic D, Veyrat-Durebex C, Lyautey J, *et al*. Divergent effects of oxytocin treatment of obese diabetic mice on adiposity and diabetes. Endocrinology 2014;155(11):4189–4201. doi:10.1210/en.2014-1466, PMID:25157455.
[28] Yoneda M, Kobayashi T, Honda Y, Ogawa Y, Kessoku T, Imajo K, *et al*. Combination of tofogliflozin and pioglitazone for NAFLD: Extension to the ToPiND randomized controlled trial. Hepatol Commun 2022;6(9):2273–2285. doi:10.1002/hep4.1993, PMID:35578445.
[29] Paternostro R, Trauner M. Current treatment of non-alcoholic fatty liver disease. J Intern Med 2022;292(2):190–204. doi:10.1111/joim.13531, PMID:35796150.
[30] Ferguson D, Finck BN. Emerging therapeutic approaches for the treatment of NAFLD and type 2 diabetes mellitus. Nat Rev Endocrinol 2021;17(8):484–

495. doi:10.1038/s41574-021-00507-z, PMID:34131333.
[31] Snider B, Geiser A, Yu XP, Beebe EC, Willency JA, Qing K, *et al*. Long-Acting and Selective Oxytocin Peptide Analogs Show Antidiabetic and Antiobesity Effects in Male Mice. J Endocr Soc 2019;3(7):1423–1444. doi:10.1210/js.2019-00004, PMID:31286109.
[32] Widmaier EP, Shah PR, Lee G. Interactions between oxytocin, glucagon and glucose in normal and streptozotocin-induced diabetic rats. Regul Pept 1991;34(3):235–249. doi:10.1016/0167-0115(91)90182-g, PMID:1924891.
[33] Gajdosechova L, Krskova K, Segarra AB, Spolcova A, Suski M, Olszanecki R, *et al*. Hypooxytocinaemia in obese Zucker rats relates to oxytocin degradation in liver and adipose tissue. J Endocrinol 2014;220(3):333–343. doi:10.1530/JOE-13-0417, PMID:24389591.
[34] Pierzynowska K, Gaffke L, Żabińska M, Cyske Z, Rintz E, Wiśniewska K, *et al*. Roles of the Oxytocin Receptor (OXTR) in Human Diseases. Int J Mol Sci 2023;24(4):3887. doi:10.3390/ijms24043887, PMID:36835321.
[35] Whitley J, Wouk K, Bauer AE, Grewen K, Gottfredson NC, Meltzer-Brody S, *et al*. Oxytocin during breastfeeding and maternal mood symptoms. Psychoneuroendocrinology 2020;113:104581. doi:10.1016/j.psyneuen.2019.104581, PMID:31911347.
[36] Maejima Y, Iwasaki Y, Yamahara Y, Kodaira M, Sedbazar U, Yada T. Peripheral oxytocin treatment ameliorates obesity by reducing food intake and visceral fat mass. Aging (Albany NY) 2011;3(12):1169–1177. doi:10.18632/aging.100408, PMID:22184277.
[37] Blevins JE, Thompson BW, Anekonda VT, Ho JM, Graham JL, Roberts ZS, *et al*. Chronic CNS oxytocin signaling preferentially induces fat loss in high-fat diet-fed rats by enhancing satiety responses and increasing lipid utilization. Am J Physiol Regul Integr Comp Physiol 2016;310(7):R640–R658. doi:10.1152/ajpregu.00220.2015, PMID:26791828.
[38] Liu CM, Spaulding MO, Rea JJ, Noble EE, Kanoski SE. Oxytocin and Food Intake Control: Neural, Behavioral, and Signaling Mechanisms. Int J Mol Sci 2021;22(19):10859. doi:10.3390/ijms221910859, PMID:34639199.
[39] Burmester V, Higgs S, Terry P. Rapid-onset anorectic effects of intranasal oxytocin in young men. Appetite 2018;130:104–109. doi:10.1016/j.appet.2018.08.003, PMID:30081055.
[40] Liu CM, Hsu TM, Suarez AN, Subramanian KS, Fatemi RA, Cortella AM, *et al*. Central oxytocin signaling inhibits food reward-motivated behaviors and VTA dopamine responses to food-predictive cues in male rats. Horm Behav 2020;126:104855. doi:10.1016/j.yhbeh.2020.104855, PMID:32991888.
[41] Attal N, Marrero E, Thompson KJ, McKillop IH. Role of AMPK-SREBP Signaling in Regulating Fatty Acid Binding-4 (FABP4) Expression following Ethanol Metabolism. Biology (Basel) 2022;11(11):1613. doi:10.3390/biology11111613, PMID:36358315.
[42] Li Y, Xu S, Mihaylova MM, Zheng B, Hou X, Jiang B, *et al*. AMPK phosphorylates and inhibits SREBP activity to attenuate hepatic steatosis and atherosclerosis in diet-induced insulin-resistant mice. Cell Metab 2011;13(4):376–388. doi:10.1016/j.cmet.2011.03.009, PMID:21459323.
[43] M Onorato A, Fiore E, Bayo J, Casali C, Fernandez-Tomé M, Rodríguez M, *et al*. SPARC inhibition accelerates NAFLD-associated hepatocellular carcinoma development by dysregulating hepatic lipid metabolism. Liver Int 2021;41(7):1677–1693. doi:10.1111/liv.14857, PMID:33641248.
[44] Xu H, Lyu X, Guo X, Yang H, Duan L, Zhu H, *et al*. Distinct AMPK-Mediated FAS/HSL Pathway Is Implicated in the Alleviating Effect of Nuciferine on Obesity and Hepatic Steatosis in HFD-Fed Mice. Nutrients 2022;14(9):1898. doi:10.3390/nu14091898, PMID:35565866.
[45] Kwon C, Sun JL, Jeong JH, Jung TW. Humanin attenuates palmitate-induced hepatic lipid accumulation and insulin resistance via AMPK-mediated suppression of the mTOR pathway. Biochem Biophys Res Commun 2020;526(2):539–545. doi:10.1016/j.bbrc.2020.03.128, PMID:32245619.
[46] Meng J, Lv Q, Sui A, Xu D, Zou T, Song M, *et al*. Hyperuricemia induces lipid disturbances by upregulating the CXCL-13 pathway. Am J Physiol Gastrointest Liver Physiol 2022;322(2):G256–G267. doi:10.1152/ajpgi.00285.2021, PMID:34935515.
[47] Garcia D, Hellberg K, Chaix A, Wallace M, Herzig S, Badur MG, *et al*. Genetic Liver-Specific AMPK Activation Protects against Diet-Induced Obesity and NAFLD. Cell Rep 2019;26(1):192–208.e6. doi:10.1016/j.celrep.2018.12.036, PMID:30605676.
[48] Zhang Z, Liu S, Qi Y, Aluo Z, Zhang L, Yu L, *et al*. Calcium supplementation relieves high-fat diet-induced liver steatosis by reducing energy metabolism and promoting lipolysis. J Nutr Biochem 2021;94:108645. doi:10.1016/j.jnutbio.2021.108645, PMID:33838230.
[49] Plessow F, Kerem L, Wronski ML, Asanza E, O'Donoghue ML, Stanford FC, *et al*. Intranasal Oxytocin for Obesity. NEJM Evid 2024;3(5):EVIDoa2300349. doi:10.1056/EVIDoa2300349, PMID:38815173.
[50] McCormack SE, Wang Z, Wade KL, Dedio A, Cilenti N, Crowley J, *et al*. A Pilot Randomized Clinical Trial of Intranasal Oxytocin to Promote Weight Loss in Individuals With Hypothalamic Obesity. J Endocr Soc 2023;7(5):bvad037. doi:10.1210/jendso/bvad037, PMID:37153702.